CONCEPTUAL DESIGN OF BUNDLE DIVERTORS

Massachusetts Institute of Technology

T. F. Yang
E. J. Rapperport
J. E. Tracey
W. Langton

D. Blackfield
A. Wan
D. B. Montgomery

Draper Laboratory
J. Fisher

General Atomic
E. T. C. Cheng

CONCEPTUAL DESIGN OF BUNDLE DIVERTORS*

Massachusetts Institute of Technology

T. F. Yang
E. J. Rapperport
J. E. Tracey
W. Langton
D. Blackfield
A. Wan
D. B. Montgomery

Draper Laboratory
J. Fisher
General Atomic
E. T. C. Cheng

TABLE OF CONTENTS

1. Introduction

It has been discussed by many authors [1,2,3,4] that bundle divertors can be greatly improved by varying the coil configurations. The designs of a bundle divertor for reactors have been discussed in detail in references [1] and [2] and were found to be feasible. However, there were still many shortcomings which needed to be resolved. Two of the major shortcomings were: that the ripple is too large, which enhances the loss of energetic particles; that the current required in the divertor coil is too large, and the divertor coils interfere with the TF coils, making the maintenance difficult. To alleviate some of these problems a short T-shaped coil configuration has been proposed by T. Yang [4] and a long T-shaped hybrid divertor has been proposed by H. Furth [5]. This divertor configuration is illustrated by Figure 1. As has been discussed in the 1979 U.S. INTOR report and in reference [4], the horizontal conductor elements will increase the divertor field required to cancel the toroidal field and will also enhance the radial component of the diverting flux lines. Such a divertor requires less current and thus produces lower ripple. Another method of reducing the ripple is to use an "X"-shaped four-coil arrangement like a small tokamak, proposed by R. Dory and John Sheffield [2]. All these configurations have been examined in this report. It is found that four coil configuration gives the lowest ripple but the associated engineering problems are quite difficult. A compromised physics and engineering solution can be obtained from the two T-shaped coil configurations.

2. Magnetic Concept

2.1 Magnetic Configuration

The plasma parameters and TF coil number and size used in this study are listed in Table 1.

Table 1. Key parameters for INTOR and ETF used in this study.

	= INTOR	ETF
R_0	= 5.2 m	5.5 m
B_0	= 4.8 T	5.5 T
a	= 1.3 m	1.4 m
R_{TF}	= 10.5 m	11.5 m
$TF\#$	= 12	12

$^*R_{TF}$ (outer radius)

These parameters are chosen partly based on the INTOR and ETF space under consideration, and partly for computational convenience. They provide information and comparison for different sizes and field intensities and a flexible range when choosing final parameters. The coil configurations studied here are shown in Figure 2. The typical flux patterns for these coil configurations except (a) are shown in Figure 3. The magnetic configuration of coil type (a) is similar to Figure 3(c). Configuration 3(b) shows the T-shaped divertor with expander coils. It shows that flux can be led to the outside of the TF coils and expanded which makes the particle removal and thermal handling easier. The configuration 3(c) was considered to be desirable for lower ripple and energetic particle containment. The major disadvantage is that the magnetic intensity at the middle of the diverted flux loop, is 17 Tesla, i.e., the field becomes the strongest and the flux tightest at this point where expansion is needed most. The 17 Tesla field makes the expansion nearly impossible. An attempt has been made to expand the flux or reduce the field intensities by opening the outer legs as shown by configuration 3(c) and by changing the coil shape as shown by Figure 3(d). The gain is insignificant. The radially outward translational force in configuration 3(b) is approximately equal to 20 MN whereas it is nearly zero in configuration 3(c). In the configuration 3(c) the interaction of the divertor with the TF coil is negligible. From an engineering point of view it is nearly an independent structure, since minimal structure is required to hold the divertor assembly in place. As will be discussed in the mechanical section, the divertor can still be designed as a plug-in unit for case (b). Lacking an adequate method to expand the flux, or to remove the particle and heat load in the very tight space in case (c) and (d), we will concentrate our effort in optimizing case (b). To determine the optimized design parameters, the field ripple on axis and the divertor current are plotted in Figures 4, 5, 6 as functions of height, width and length, while the coil position and separatrix are fixed. Figure 7 plots the ripple and the position of the separatrix as function of current. The design point for INTOR is shown by the dot. The

3

choice was made based on many engineering and physics considerations. For physics consideration one would like to make the ripple as small as possible. The ripple reduces linearly as the width reduces and the length increases. However, the current requirement increases in both cases. The ripple and current decrease with the height and there is obviously no lower bound. Therefore, physical contraints have to be considered for making the selection of parameters.

For the convenience of maintenance, the width of the divertor assembly was chosen to be smaller than the gap so that the whole assembly can be removed without interfering with the TF coils. The width and height are also the minimum required to allow 30 cm of shielding on each side, 30 cm of plasma duct, 50 cm of conductor pack, and 10 cm of structure. The amount of shielding chosen is based on the life time of 1 MW-Year. Anything less is considered dangerously optimistic.

The magnetic field intensitites along a field line of the midplane for the two T-coil case are shown in Figure 8. The ripples calculated from these fields are plotted as a function of major radius and shown in Figure 9. Figure 10 shows the ripple as a function of vertical distance z from the midplane for fixed radii. The ripple curves can be approximated by an exponential function

$$E(z, R) = E_o(R)e^{-z^2}/a,$$

where $a = 1.06$ for this particular case and $E_o(R)$ is the amplitude of the ripple given in Figure 10. The expanded ripple for T-coil with expander and for the four-coil type is also plotted in Figure 9. The ripple for the T-coil with expander is only 0.4 on axis and becomes positive at a smaller radius and is generally better than the four-coil case. The implication of this kind of ripple distribution on the particle confinement has to be studied. Preliminary calculations of an α-particle orbit and beam particles are given in the following section.

2.2 α-Particle Confinement

The α-particle orbits have been studied for four cases using the code FLOC developed by Fowler and Rome [6]. In Case 1,the current is 7.2 MA and the divertor height-to-width ratio is 0.58; the orbit is shown in Figure 11, and the banana orbit is not confined. In Case 2, the current is 8.3 MA and the height-to-width ratio is 0.5, but the coils are separated by 1.4 m. The banana orbit is again not confined as shown in Figure 11. In Cases 3 and 4, the height-to-width ratio is 0.5 and the coils are separated by 1.2 m, and the divertor currents are 11.2

MA-T and 6.72 MA-T respectively. In both cases the α-particles are confined as is shown in Figure 12. The time sequence of the banana shows that the banana steps toward the center of the machine. More study is required in order to draw a positive conclusion. However, the results indicate that the α-particle can be confined for such a divertor system. The typical confined beam particle orbit is shown in Figure 13. The lower picture shows the variation of angular momentum of which is time average is nearly conserved.

3. Structural Concept of ETF Bundle Divertor

A prime requirement of the structure is the necessity to provide easy demounting of the bundle divertor from between the TF coils for servicing requirements.

Four "L"-shaped saddle magnet coils, each approximately 50 cm square in cross-section, 2.4 meters high, 1.2 meters wide, and 1.2 meters long are arranged to form a bundle divertor for the INTOR. These coils may be constructed of OFHC water-cooled copper conductors run at a current density of less than 6000 a/cm^2 in the conductor. The substantial forces generated by these windings are delivered to their surrounding structure in three dimensions. Hence, the structure conceived is made extremely stiff in all three dimensions.

3.1 Forces

The net horizontal plane forces delivered by the divertor coils to their containment structure is given in Figure 14. This figure shows an indicated net radial force of about 30 MN on the whole assembly.

In addition to this net radial force, each pair of coils has substantial opposing forces in the perpendicular circumferential direction, and also in the perpendicular axial direction (out of plane). These forces have been given preliminary examination as have the interactive forces on the adjacent four TF coils.

5

3.2 Structure Concept

The basic structure containing the bundle divertor coil forces consists of two thick 304L stainless steel plates (approximately 15 cm thick) top and bottom, with built-up box beams (keyed and/or welded) of 304L stainless steel. A mid-plane section of a plan view is shown in Figure 15. The box beam sections shown in Figure 15 are schematic in nature, but they do have a geometry that keeps the bending stresses below 20,000 psi, consistent with the ASTM Boiler and Pressure Vessel Code, Section VIII, Division 2.

The four bundle divertor coils are envisioned as being sandwiched between the stainless steel plates mentioned above, with suitable intermediate tie-downs and strong-back cross-beams, to form a large, rigid monolithic assembly which fits between two adjacent TF coils as shown in Figure 16. Keyed joints (demountable) will be made between the monolithic assembly at its edges, and mating plates attached to the two TF coils to support the approximately 16 million pound net radial thrust of the divertor asssembly. The keyed joints are designed to allow remote removal of the keys and shim plates, which would then permit the radial movement of the entire monolithic divertor assembly outward from its operating position on rails, rollers, or other means.

The stainless steel plates which remain with the TF coil assemblies will have low thermal conductivity compressive links of G-10 in order to effect a satisfactory load link between the TF coils at liquid helium temperature and the divertor at ambient temperature. This compressive load link will have an intermediate liquid nitrogen cooled metallic intercept station to reduce the heat loss along the load path.

3.3 Conductor Consideration

Water-cooled copper conductors have been considered for use in the INTOR and ETF bundle divertor. Preliminary examination indicates that the 8.5×10^6 amp. turns required for each divertor coil can be achieved using a conventional square O.D. conductor (2.3 cm on a side) with a round cooling hole (1.3 cm). For the 400 turns per coil envisioned, the current in each conductor would be approximately 21,250 amperes at a current density of about 5400 amps/cm² in the conductor (3400 amps/cm² average within the coil envelope).

Half-turn (360 cm) cooling with a water flow velocity of 4.6 m/sec (approximately equal to 36.3 litres per minute per half turn) gives rise to a temperature increase of about 39°C to the cooling water at a pressure differential of about 0.79 Atm between inlet and outlet.

6

Alternatively, full-turn (7.2 m) cooling could be utilized with a water flow velocity of 9.2 m/sec (approximately equal to 72.3 litres per minute per turn) with the same 39°C temperature rise inlet to outlet and a pressure differential of about 5.5 Atm inlet to outlet.

Each front coil, therefore, requires approximately 70 MW of electric power for its operation and about 28,766 litres of water per minute to remove this power. The power requirement for half height coil and current 6.72 MA-T would be approximately 33 MW.

4. Nuclear Shielding Study

A one-dimensional ANISN calculation has been done to estimate the shielding thickness needed for the normal conduction operation. The one-dimensional shield model is shown in Figure 17. The dose rate on the insulation material (epoxy-base material such as G-10) as a function of shield thickness for three shield material combinations, 10% H_2O (B) + 50% W, 30% H_2O (B) + 70% W and 50% H_2O (B) + 50% W have been obtained. The results show that the 10% H_2O (B) + 90% W shield is the best material combination. The neutron flux, nuclear heating and dose rate are plotted in Figures 18, 19, and 20, as functions of thickness for the best case.

The dosage on the insulator can be expressed as

$$D(x) = D(o)e^{-0.14008t - 3.3333 \times 10^{-4}t^2},$$

where $D(o) = 2.5 \times 10^{11}$ Gray/year at MW/m^2 wall loading and t is the shield thickness with unit measure of cm. The lifetime of the insulation for three thicknesses for the dose limits of 10^7 and 10^9 Grays are listed in Table 2. Since there is 10 cm structure and 30 cm shielding, it is fair to say that the divertor can operate for 1 MW-Yr/m^2. If the duty factor is 50%, the divertor lifetime would be one year for 2 MW/m^2 wall loading. Since the divertor can be designed as a plug-in unit, a one-year replacement schedule should be very reasonable.

Table 2. Magnet Lifetime ($MW \cdot YR/m^2$) for Dose Limits of 10^7 and 10^9 Grays.

Shield Thickness		Insulation Dose Limits
cm	10^7 Gray	10^9 Gray (MIT test)[7]
30 cm	0.004	0.4
40 cm	0.02	2
50 cm	0.1	10
60 cm	~ 1	100

5. Summary and Discussion

The coil dimensions, current and power consumption are listed in Table 3.

Table 3.   Dimensions and Currents for Selected Bundle Divertor for INTOR

$height = 1.40$ m	$I_1 = 6.72$ MA-turns
$length = 1.20$ m	$I_2 = 4.8$ MA-turns
$R_1 = 7.3$ m	coil cross-section $= 50 \times 50$ cm
$R_2 = 10.2$ m	Average $j = 2.6$ ka/cm^2
	$= 0.56$ ka/cm^2/Tesla

The current required for ETF is 8.3 MA-T and $R_1 = 7.6$ m. This divertor is feasible from an engineering and physics standpoint; the power consumption and lifetime are reasonable, and the replacement is easy. The most significant achievement of this concept is the drastic reduction in size and outboard forces. This fact can be demonstrated by the comparison of INTOR and ETF with a similar reactor design DTHR( ) as is shown in Figure 21. DTHR uses conventional two coil divertor whose size is more than double that of INTOR and ETF. Further optimism and detailed study of particle confinement are in progress.

8

References

1. T. F. Yang et al, 8th Symposium, IEEE, San Francisco (1979).

2. John Sheffield, R. A. Dory, "The Ripple Bundle Divertor for Tokamaks", ORNL-TM6220 (March, 1978) and U. S. INTOR Report (1979).

3. A. D. Sanderson, P. E. Stott, "A Bundle Divertor for Fusion Reactor", CLM-P530, Culham Laboratory, Abingdon, Oxfordale, England (1978).

4. T. F. Yang, U. S. INTOR Report (1979) and Westinghouse Report (1980) "Bundle Divertor Magnetics for ISX-B, ETF and Reactors" pro. of the U. S./Japan Workshop on Divertors, 1st Wall Materials and Impurity Control, JAERI-M8971 Japan, (March, 1980) P. 165.

5. H. Furth, C. Ludescher, U. S. INTOR Report (1979).

6. R. Fowler and J. Rome, FLOC code.

Conductors

Null Trace

Fig. 1 Schematic of a T-shaped bundle divertor coil.

(a)
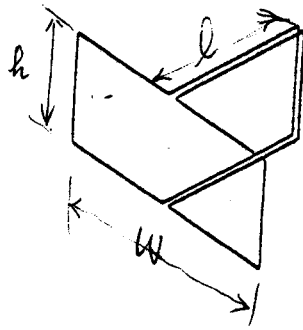
(b)
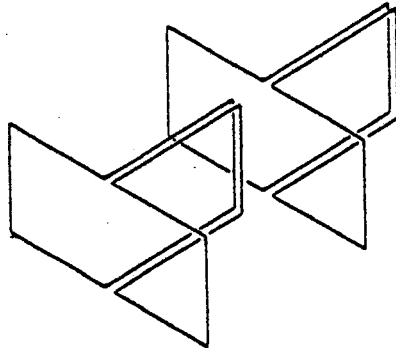
(c)
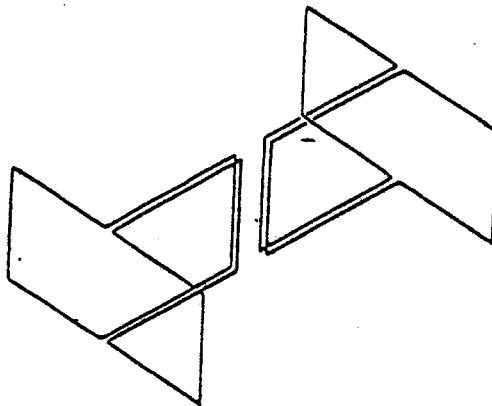
(d)
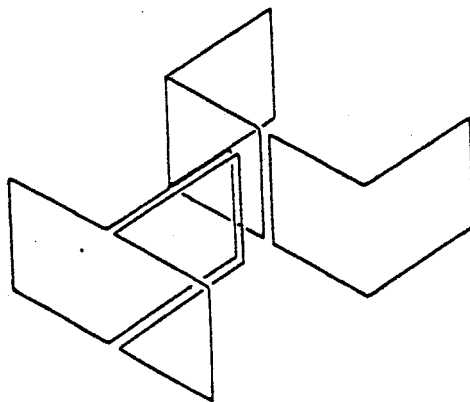
Figure 2   Divertor Coil Configurations
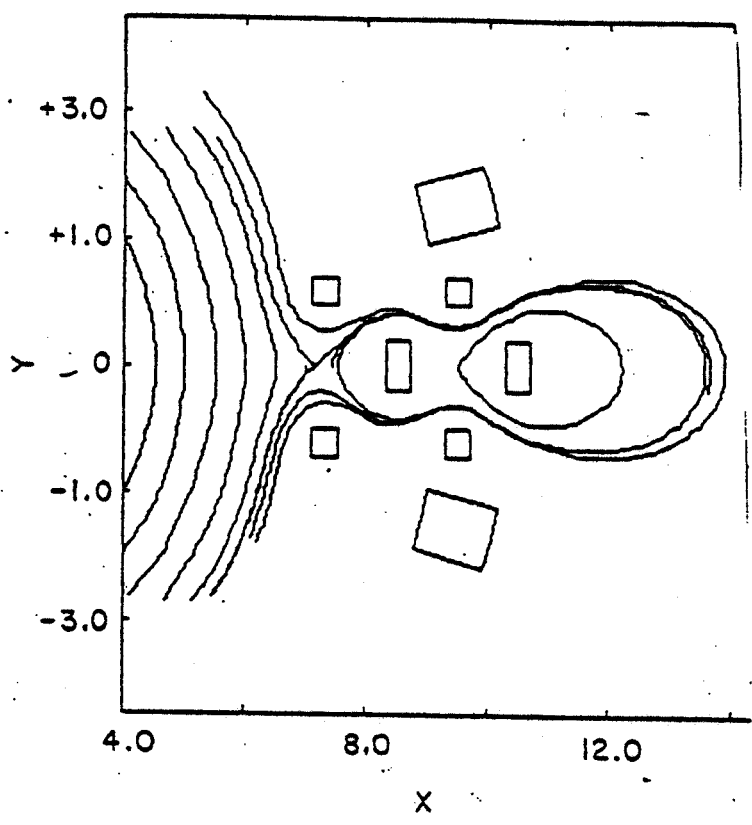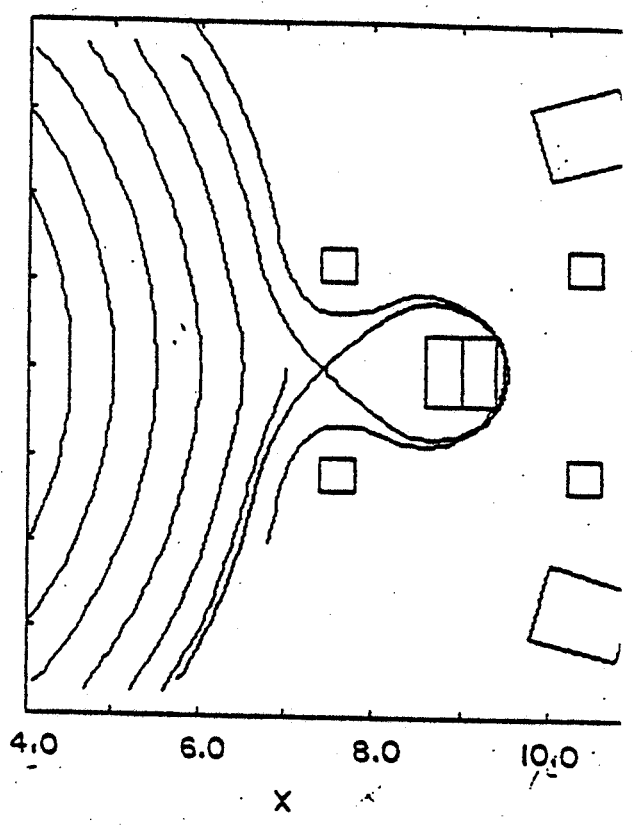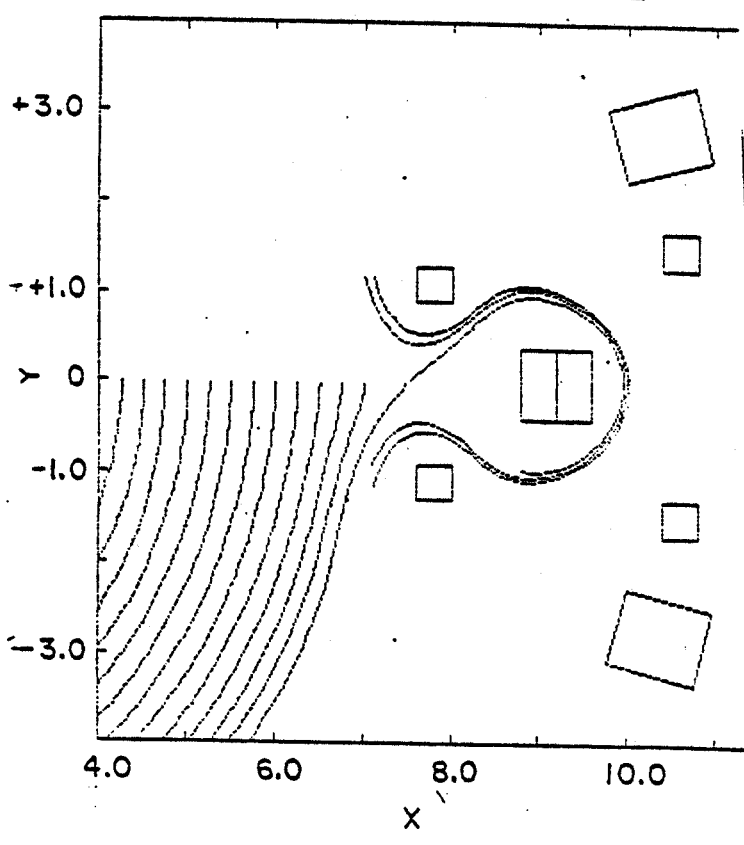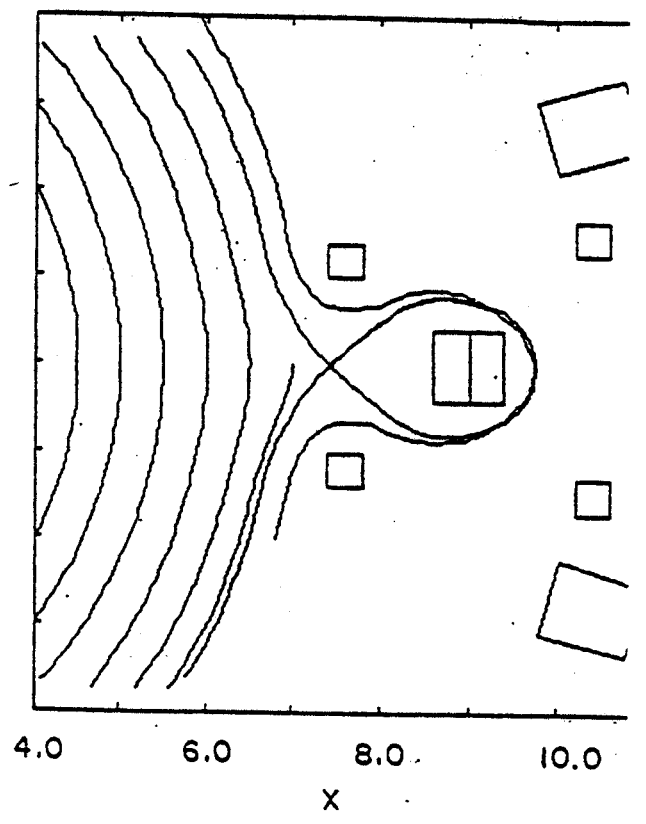
Figure 3   Magnetic Flux Configurations for the
            coil type (b), (c), (d) and (e) in
            Figure 2.   3.10
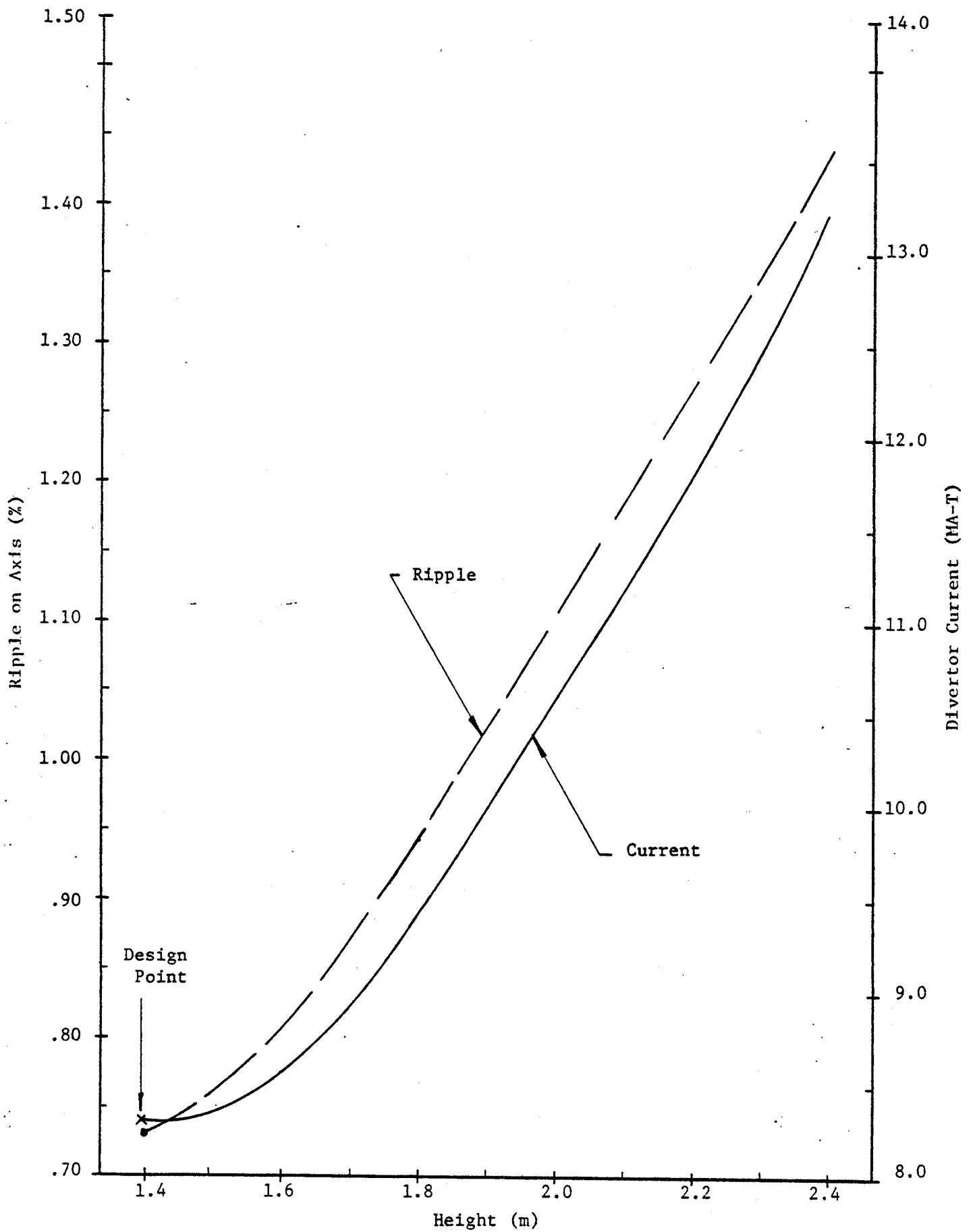
Figure 4   Both ripple and current increase with height.
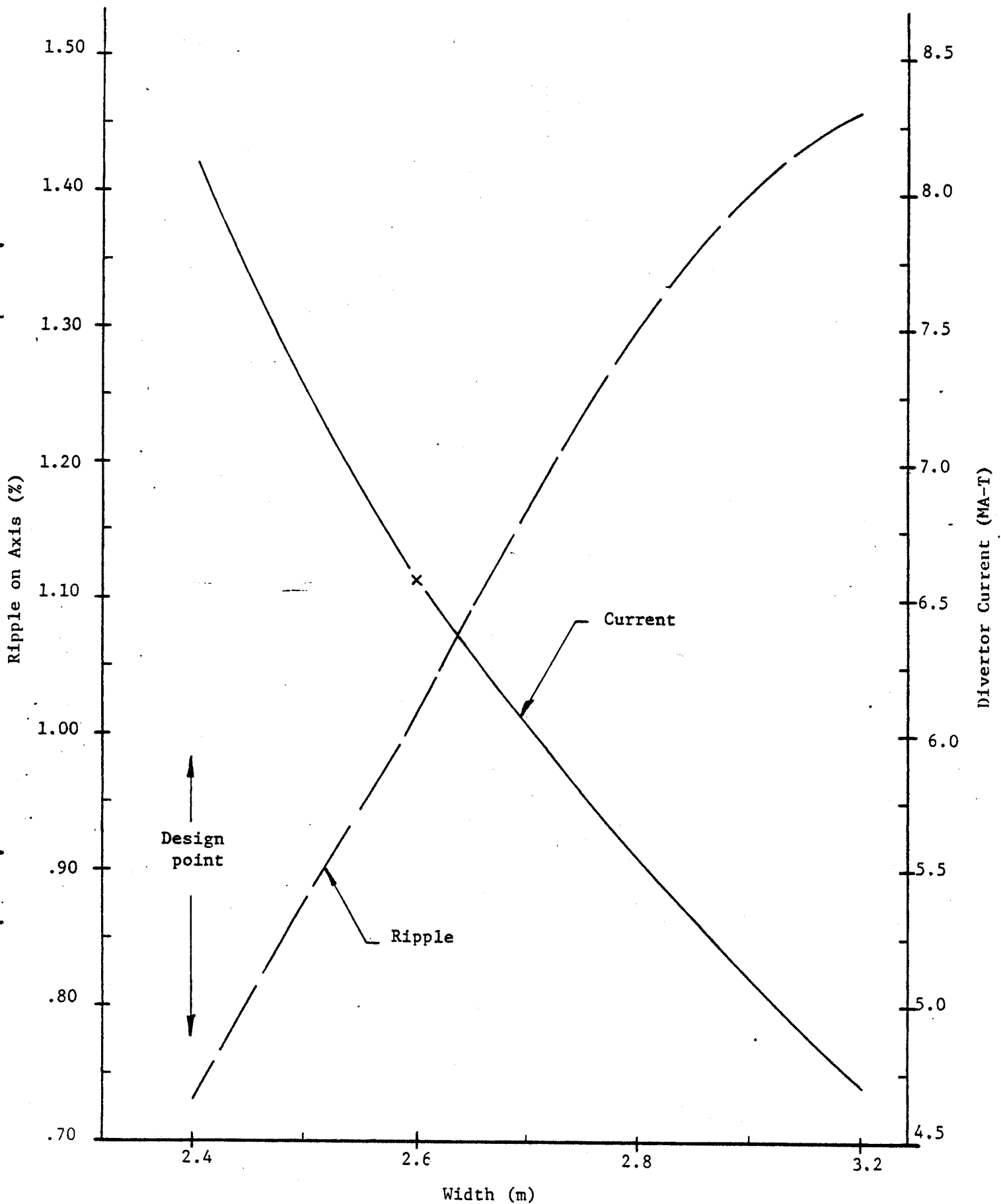
Figure 5   Ripple and current as functions of width
(Ripple increases while current decreases with width)
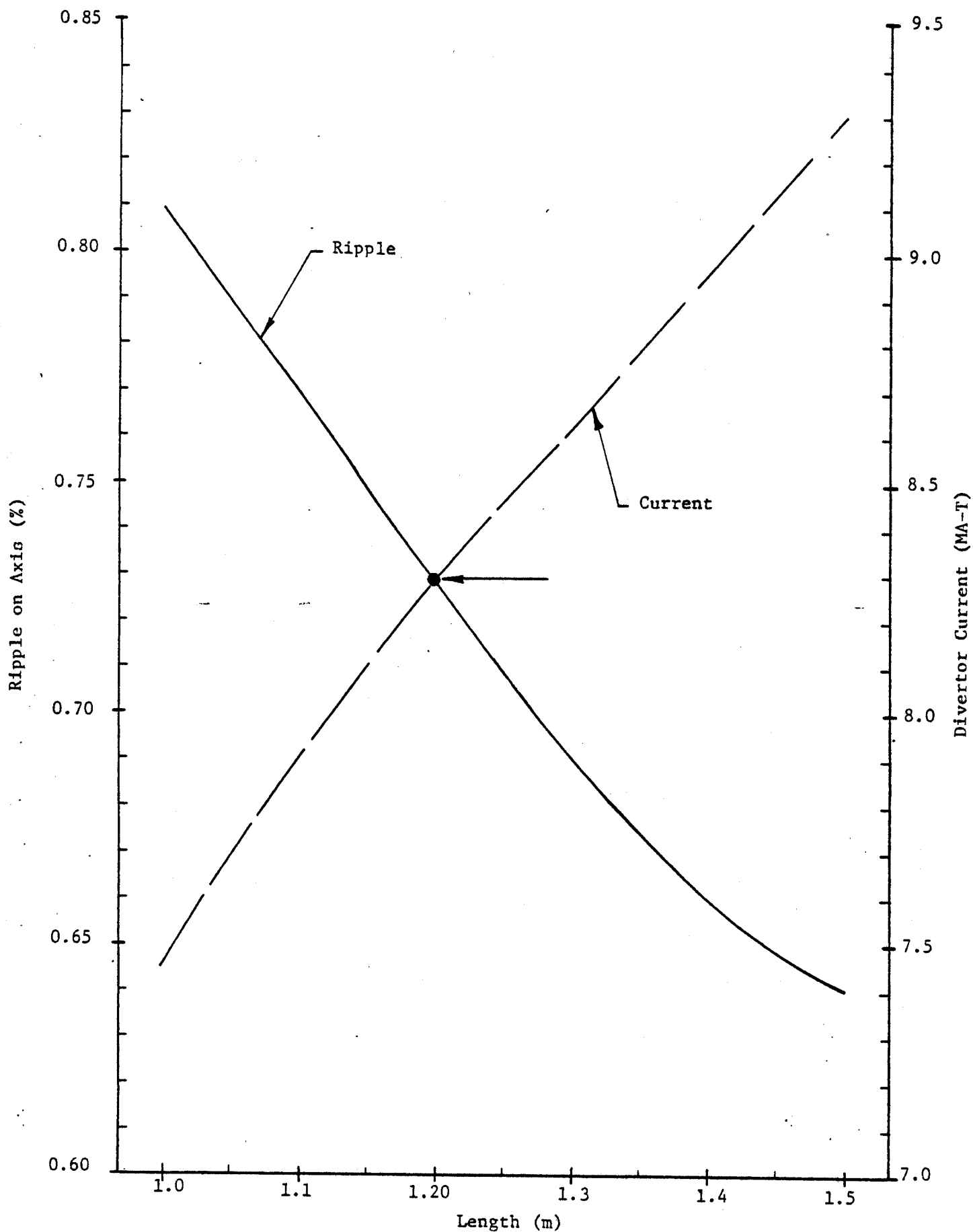
Figure 6   Ripple and current as functions of length
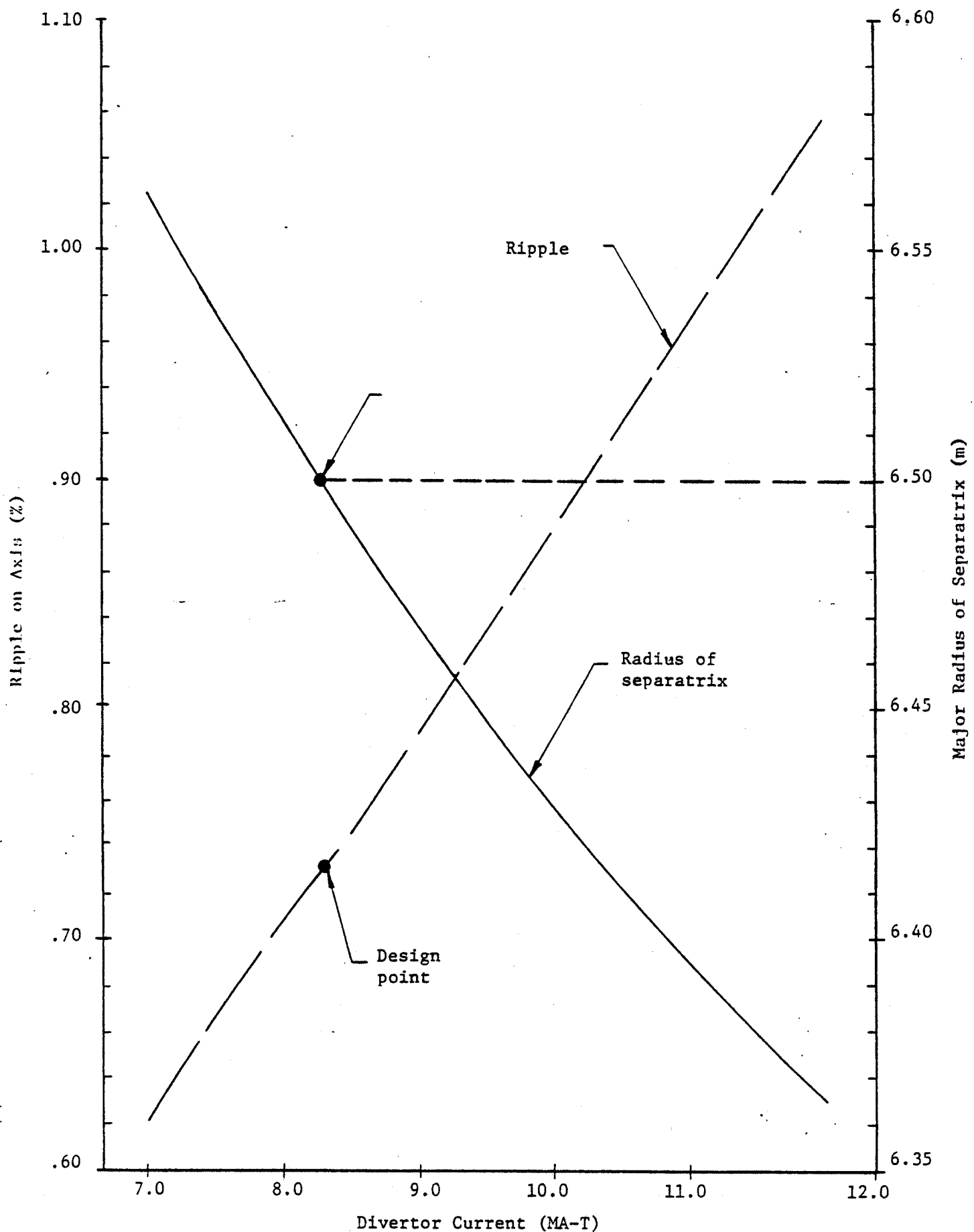
Figure 7   Ripple and radius of separatrix as function of current.

dxpetf5bf1
frame: 3
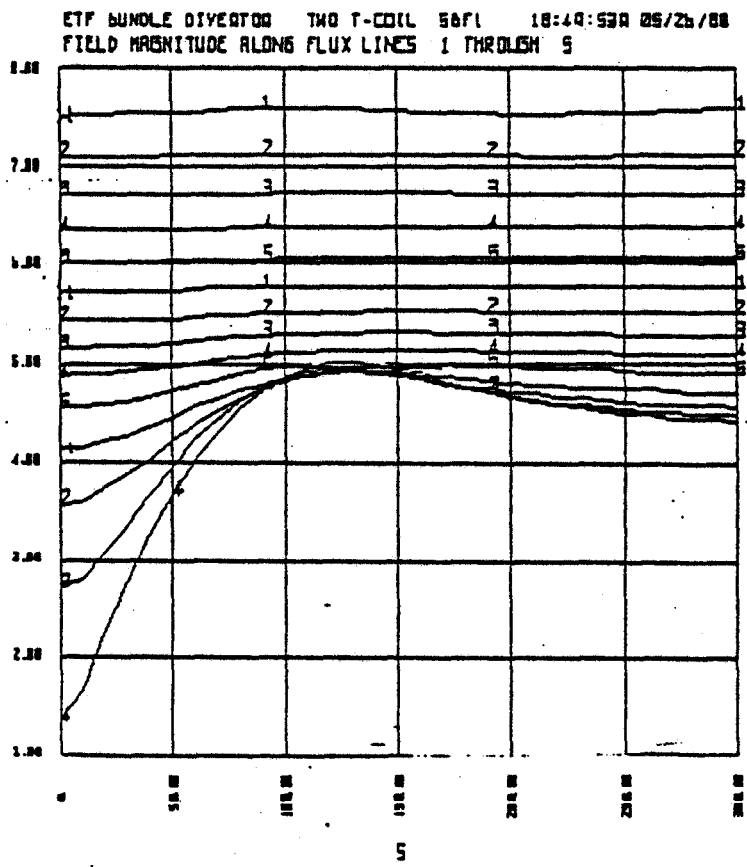
Figure 8   Field Intensities along the Field
            Line for Configuration 3C.

$$|\Delta B| = \left|\frac{Bmax - Bmin}{Bmax + Bmin}\right|$$

ALONG FIELD LINES

R	%
-75	.254
-50	.360
-25	-.095
0	-.398
25	-.837
50	-1.54
75	-2.88
100	-5.43
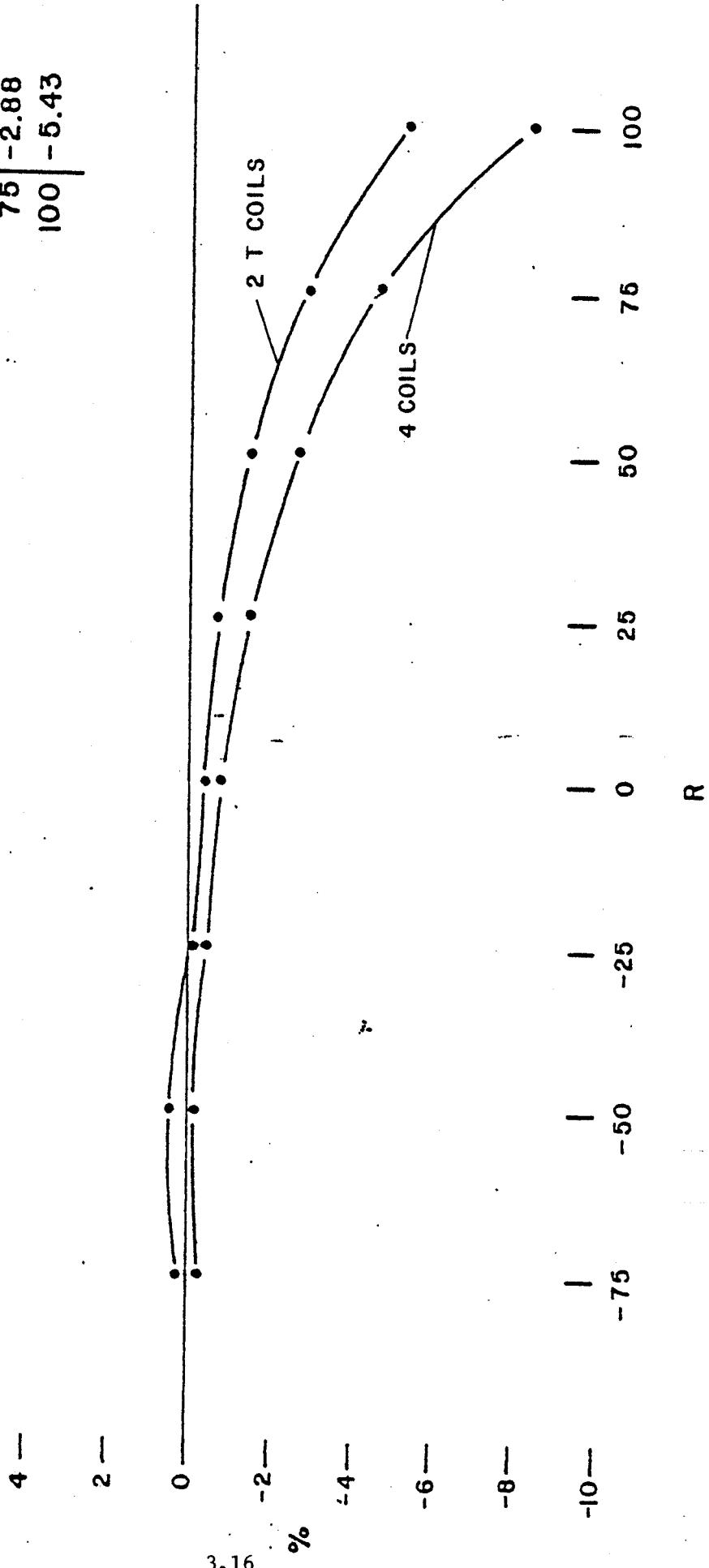
Figure 9   Comparison of ripple for 4 coils and one T with expansion coils.
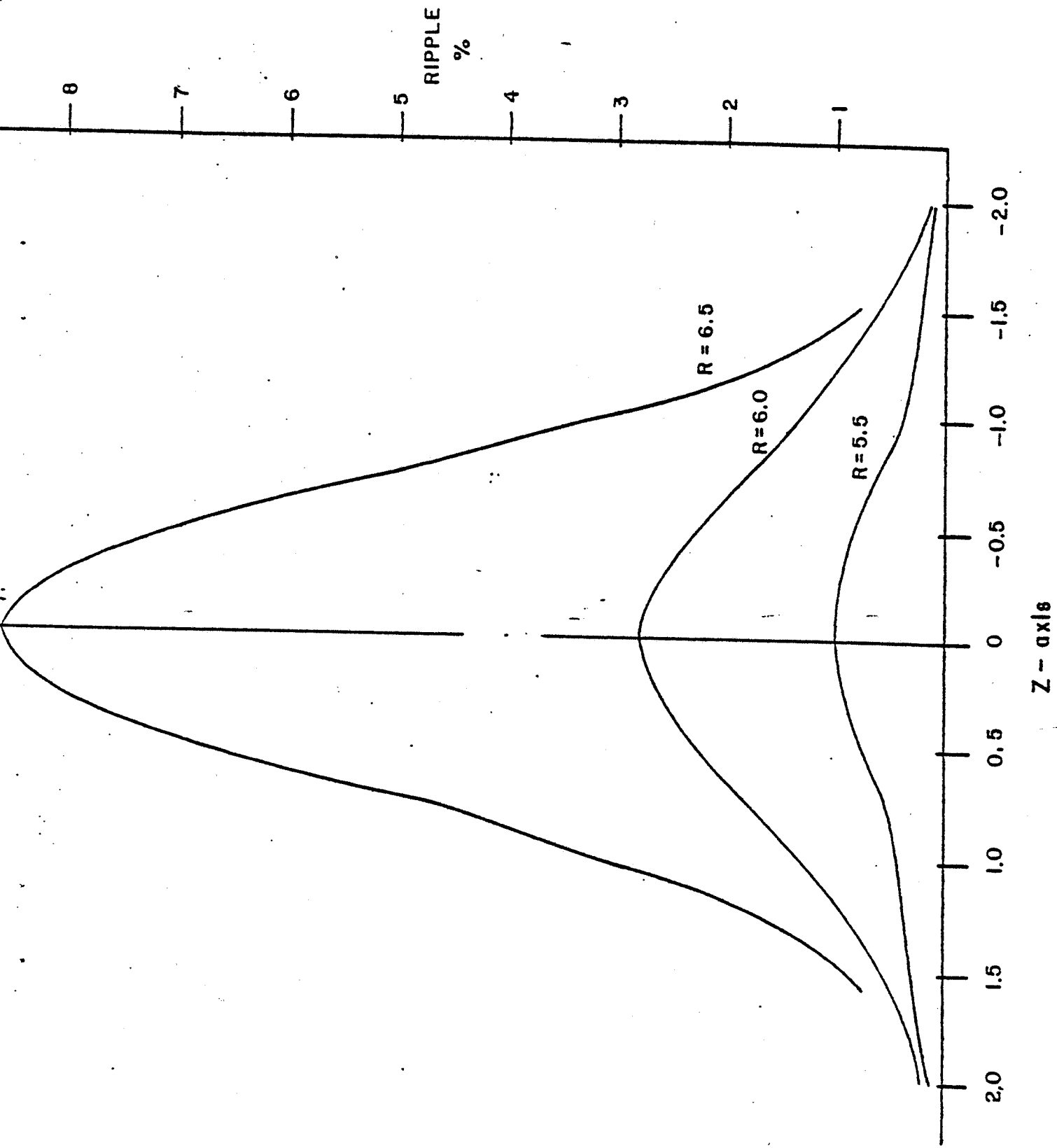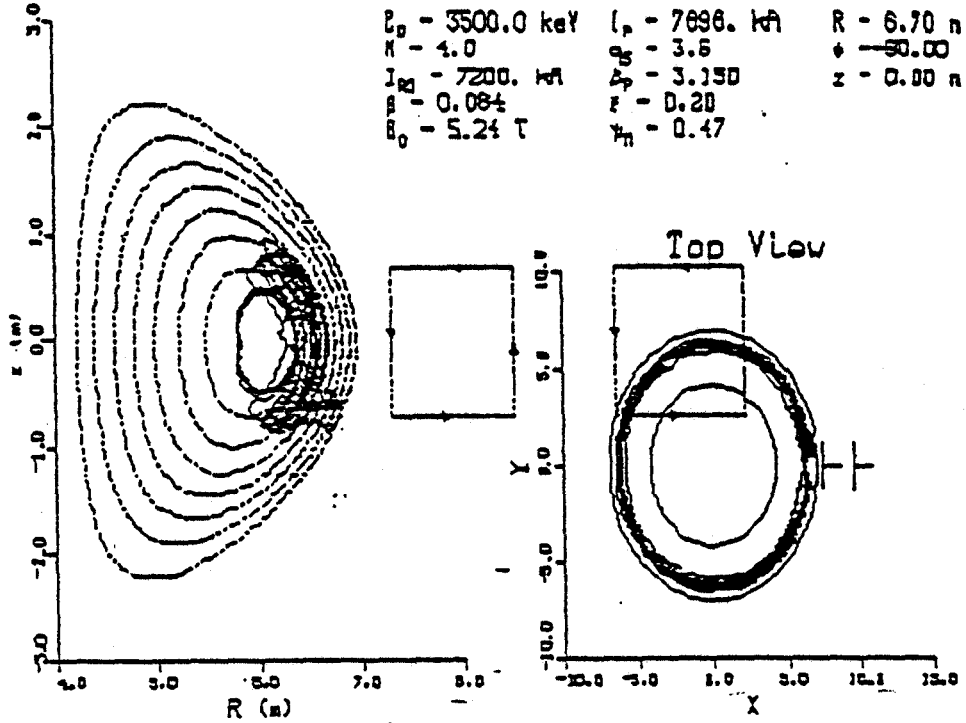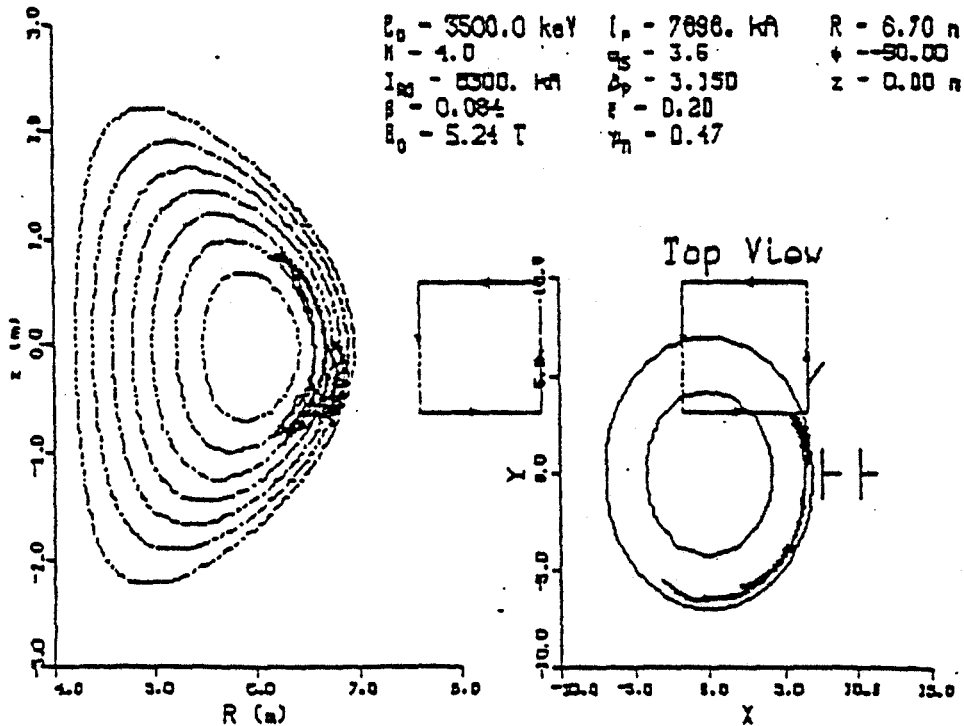
3.16

RIPPLE %

8

7

6

5

4

3

2

1

R = 6.5

R = 6.0

R = 5.5

Z – axis

-2.0

-1.5

-1.0

-0.5

0

0.5

1.0

1.5

2.0

3.17

Figure 11 Unconfined α-particle orbits.
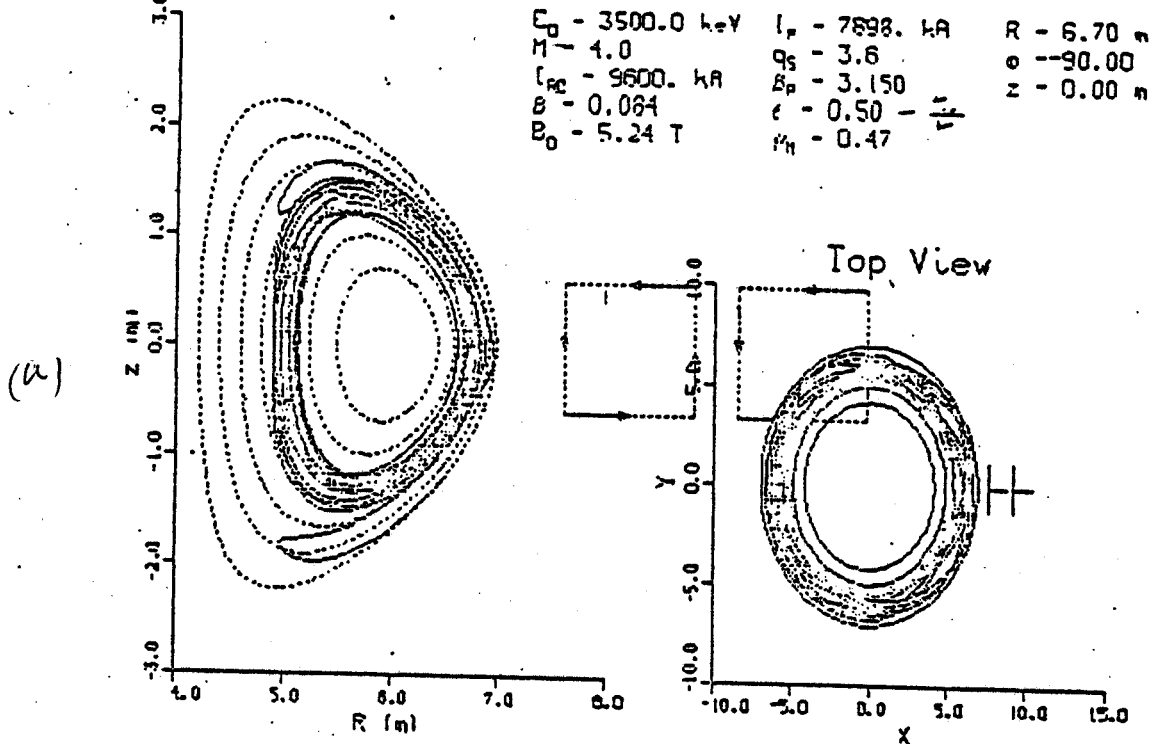
GUIDING CENTER ORBIT

E_0 - 3500.0 keV I_p - 7898. kA   R - 6.70 m
M - 4.0 q_s - 3.6   o - -90.00
I_{PC} - 9600. kA B_p - 3.150   z - 0.00 m
β - 0.084 ℓ - 0.50
B_0 - 5.24 T r_n - 0.47

Top View

(a)

GUIDING CENTER ORBIT

E_0 - 3500.0 keV I_p - 7898. kA   R - 6.70 n
N - 4.0 q_s - 3.6 ϕ - -90.00
I_{PO} - 6700. kA B_p - 3.150   z - 0.00 n
β - 0.084 ℓ - 0.20
B_0 - 5.24 T r_n - 0.47

Top View

(b)

Figure 12   Confined α-particle orbits

GUIDING CENTER ORBIT

E_0 – 150.0 keV I_P – 4900. kA   R – 6.50 m
M – 2.0 q_S – 4.3 ϕ – –90.00
I_{RC} – 8000. kA β_P – 0.532   z – 0.00 m
β – 0.006 ε – 0.50
B_0 – 5.50 T ψ_M – 0.74

Top View
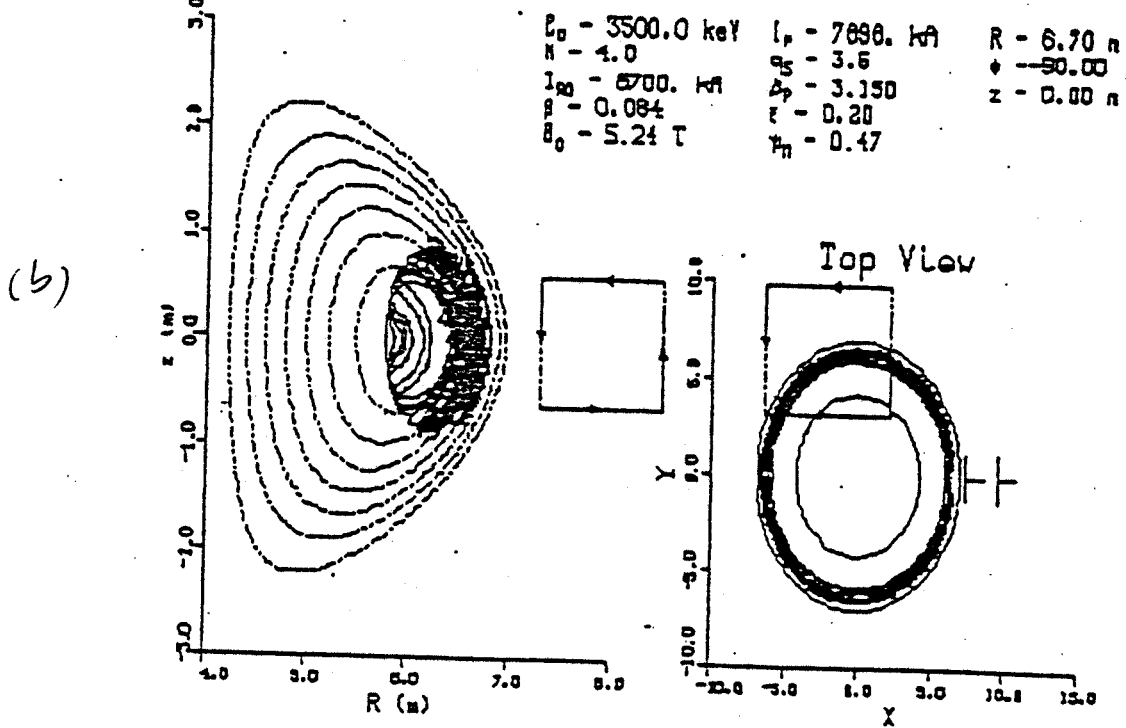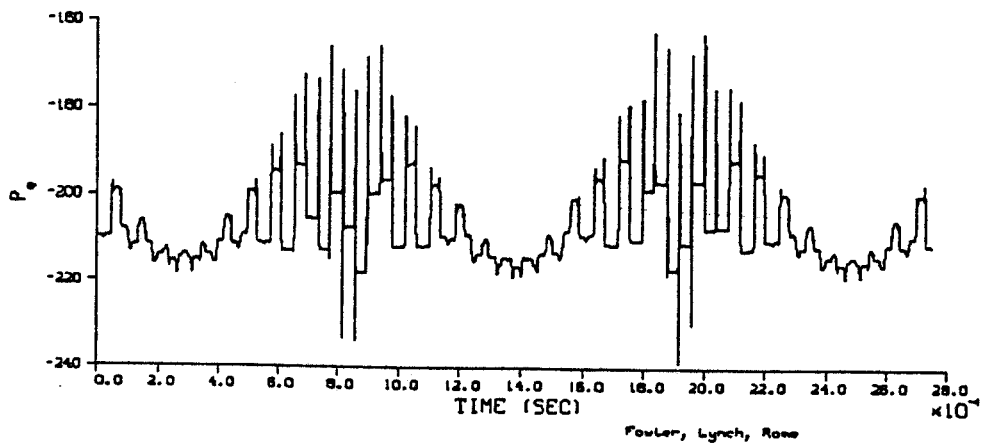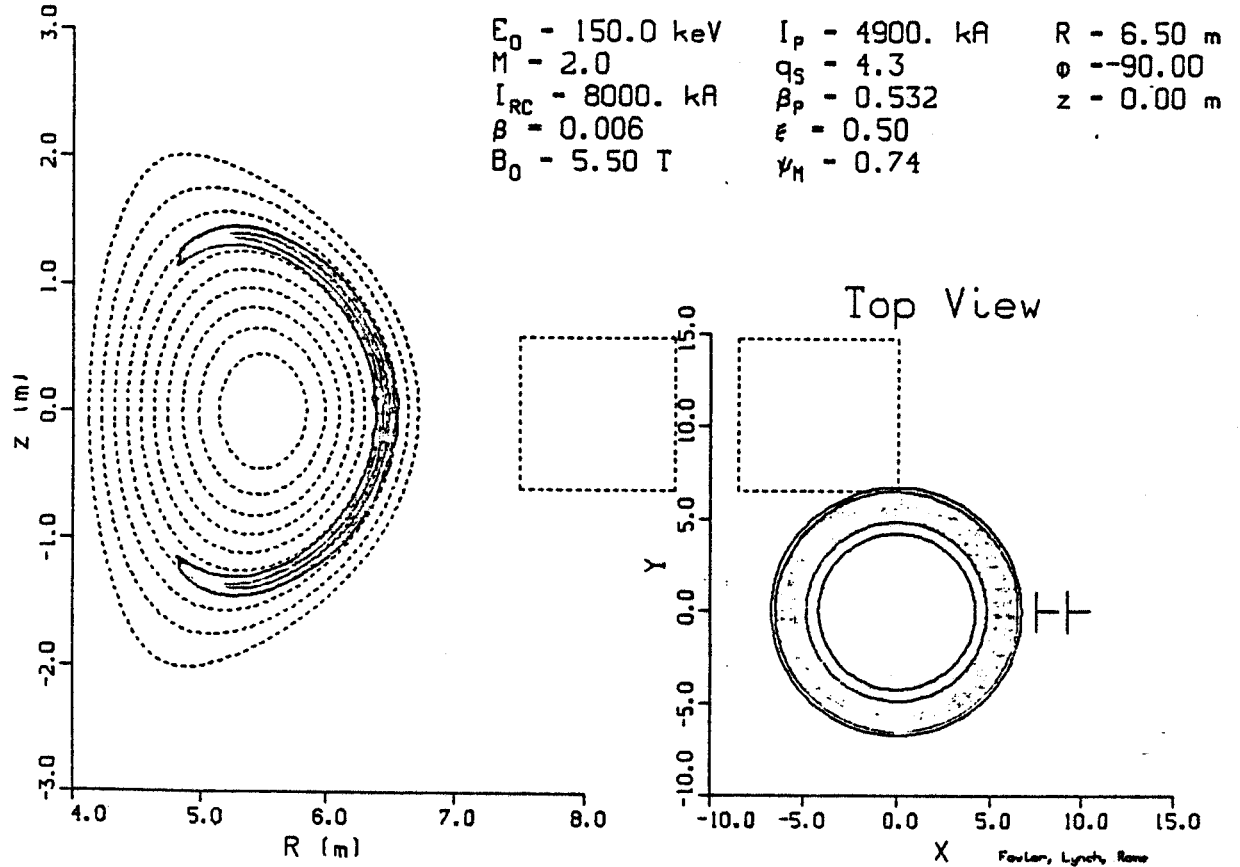
Figure 13   Typical confined beam particle
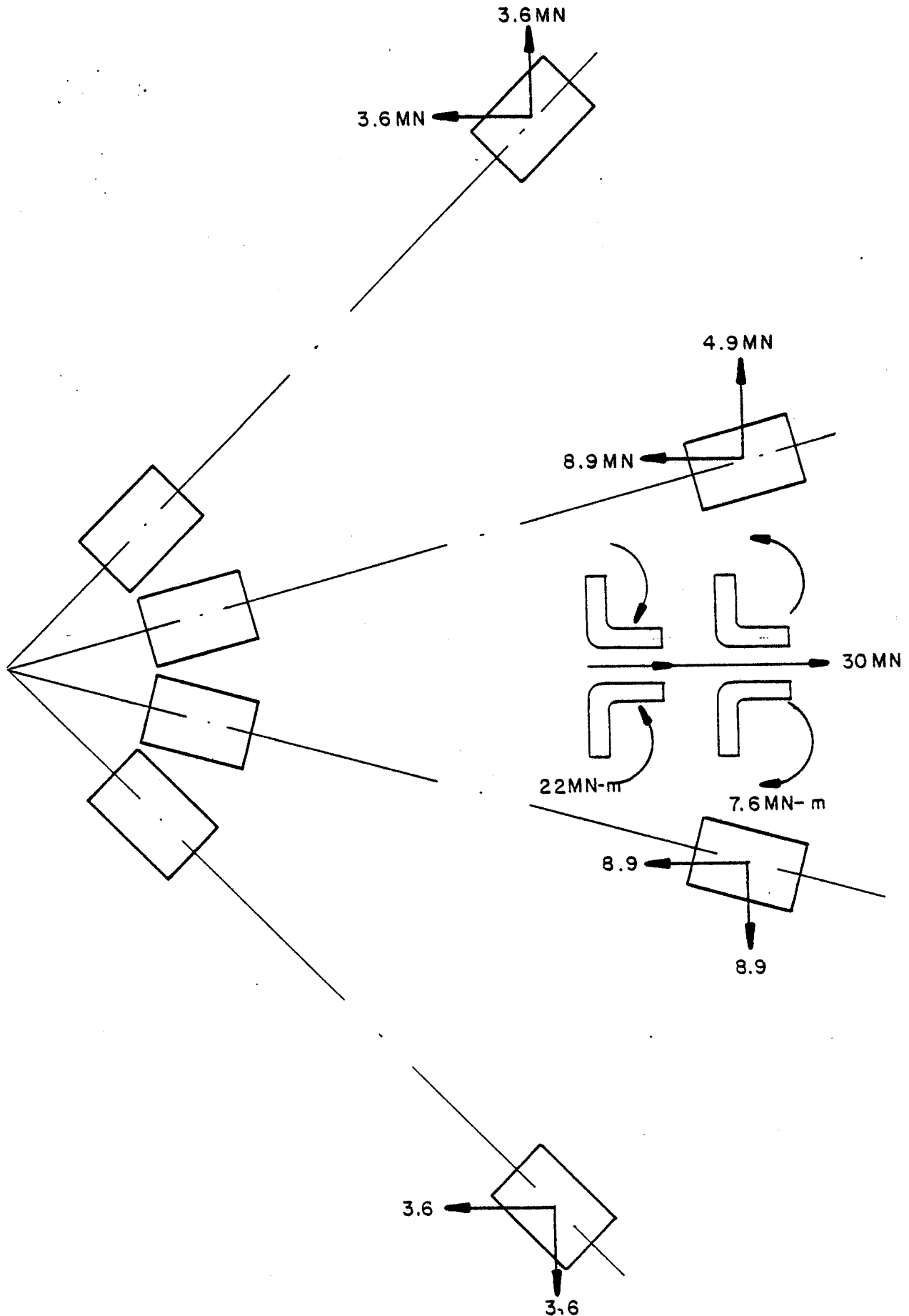
Figure 14   Preliminary summation of forces acting on energized
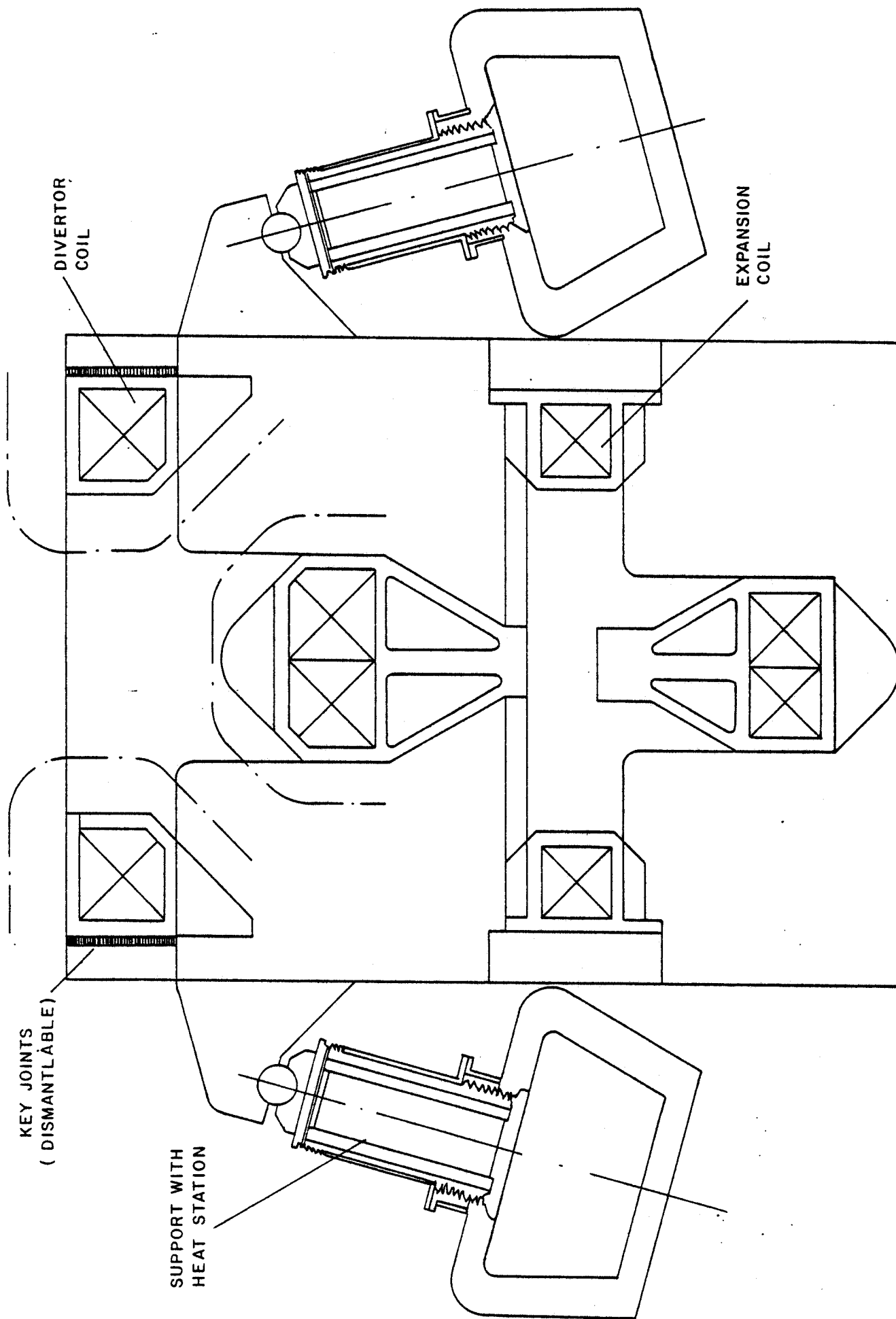bundle divertor coils of INTOR.

3.21

DIVERTOR COIL

EXPANSION COIL

KEY JOINTS (DISMANTLABLE)

SUPPORT WITH HEAT STATION

Figure 15   INTOR and ETF bundle divertor coils with

3.22

ETF
BUNDLE
DIVERTOR

TF COIL

EXPANSION
COIL

DIVERTOR
CONTAINMENT
STRUCTURE
(MONOLITHIC CRATE)

TF COIL

COMPRESSIVE
SUPPORT

JET-M.I.T.

RADIAL
RESTRAINT
BEAM
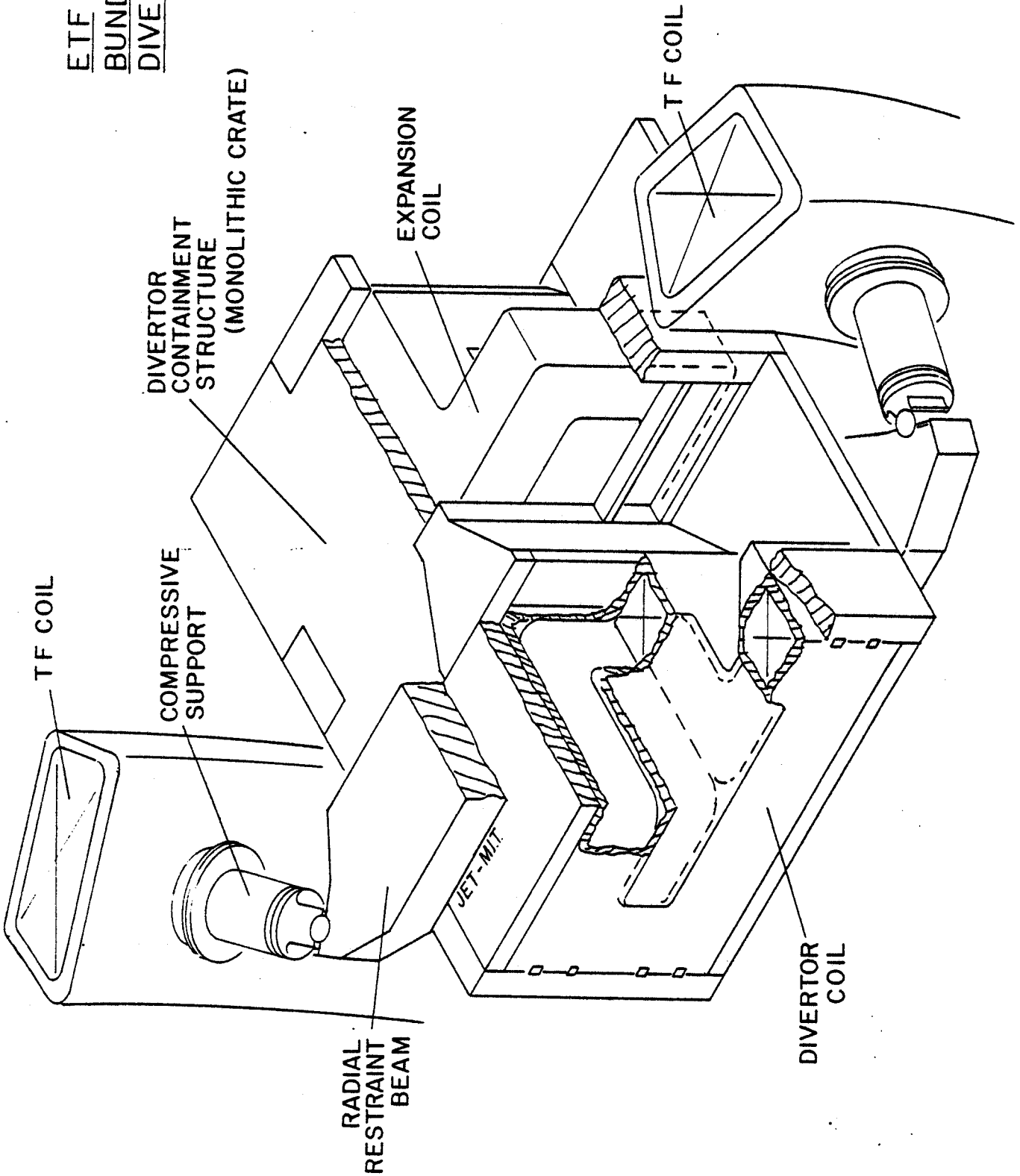
DIVERTOR
COIL

Figure 16   INTOR and ETF bundle divertor assembly

ONE-DIMENSIONAL SHIELD MODEL
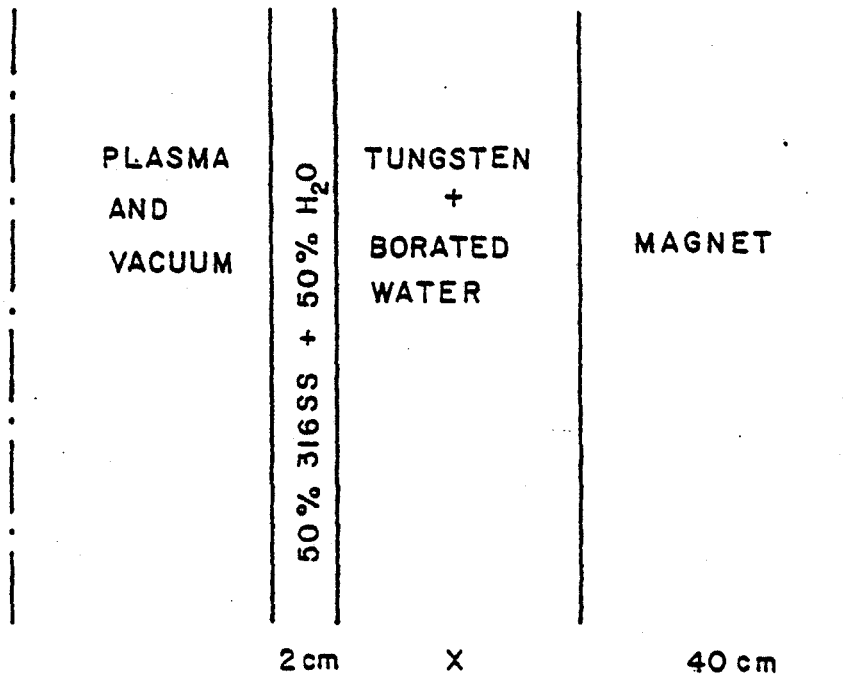
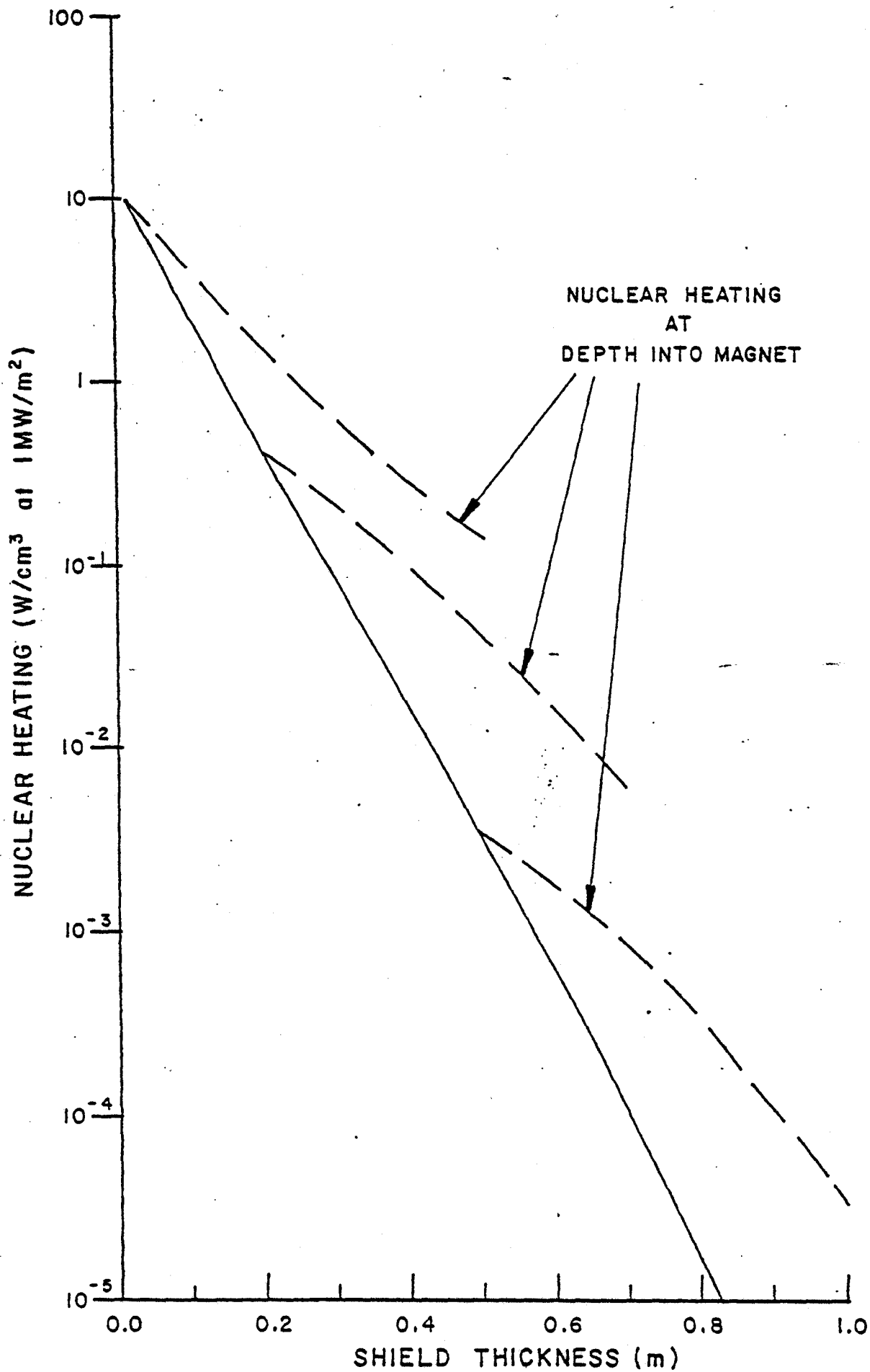Figure 17   One-dimensional shield model
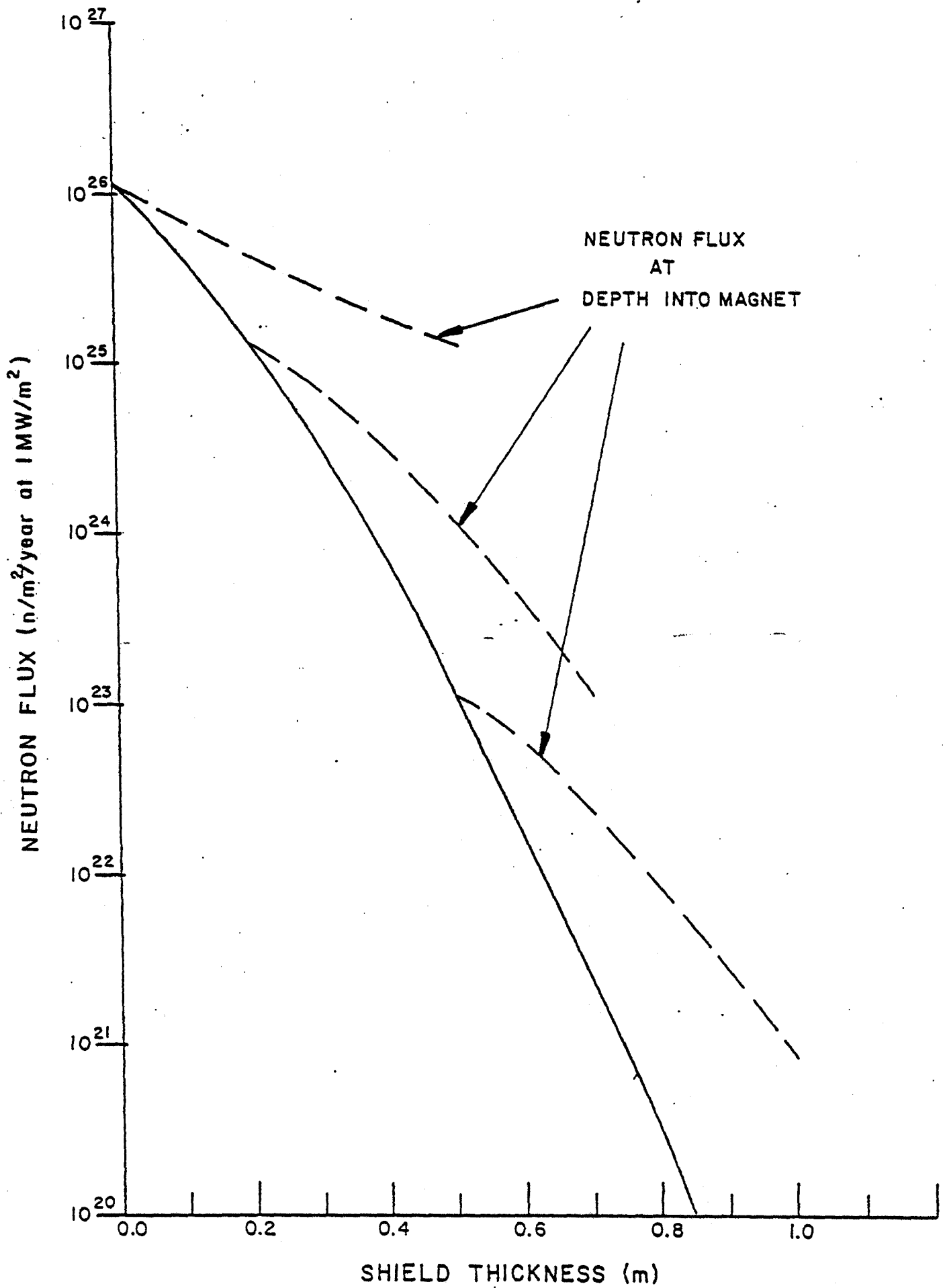
Figure 18   Neutron flux as function shield thickness

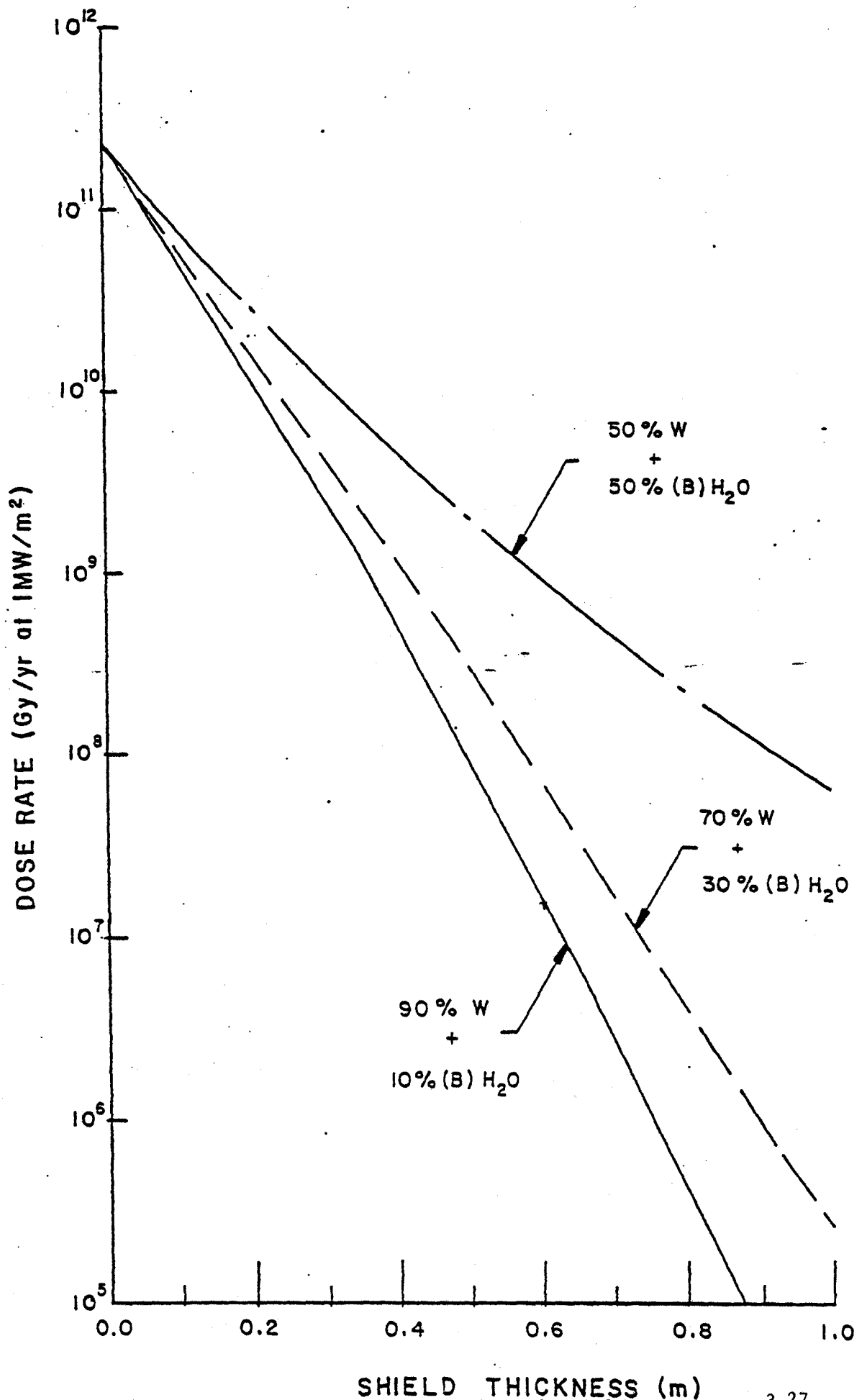Figure 19   Nuclear heating as function of shield thickness

3.26

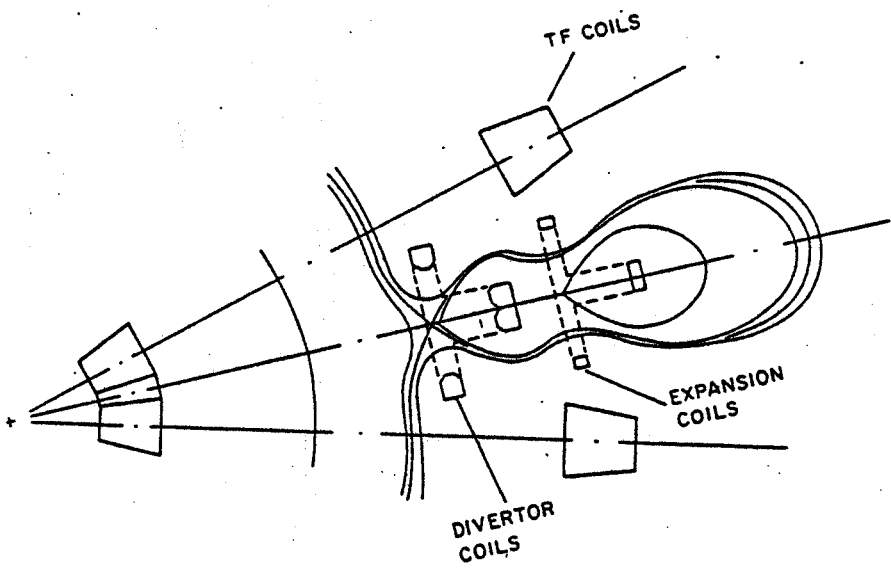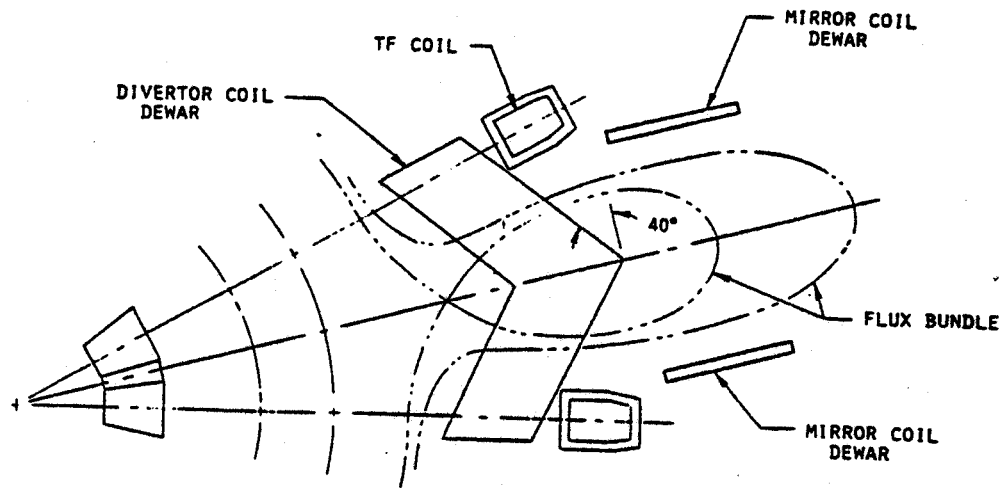Figure 20 Dose rate as function of shield thickness   3.27

Figure 21   Comparison of two circular coil divertors
and two T-shaped coil divertors

3.28